SEMARAK ILMU PUBLISHING

CFD Letters

Journal homepage:
https://semarakilmu.com.my/journals/index.php/CFD_Letters/index
ISSN: 2180-1363

Numerical Study of Resistance Trimaran Unmanned Surface Vehicle Based on NACA Foil

Fajri Ashfi Rayhan[1,*], Saiful Fadillah[1], Arya Khairullah Akbar[1], Bima Anugerah Putra[1], Amir Marasabessy[1], Reda Rizal[2]

[1] Naval Architecture and Marine Engineering, Faculty of Engineering, Universitas Pembangunan Nasional "Veteran" Jakarta, 12450, Jakarta, Indonesia
[2] Industry Engineering, Faculty of Engineering, Universitas Pembangunan Nasional "Veteran" Jakarta, 12450, Jakarta, Indonesia

ARTICLE INFO

Article history:
Received 18 April 2023
Received in revised form 15 May 2023
Accepted 16 June 2023
Available online 1 November 2023

Keywords:
Unmanned Surface Vehicle; Resistance; Trimaran; NACA

ABSTRACT

Unmanned Surface Vehicles (USVs) are used to monitor territorial waters and collect sea data, including hydrographic and oceanographic data. Compared with larger survey vessels, USVs are more flexible and cost-efficient because of their compact form. The latest USV design uses NACA foil as a trimaran hull form with a self-maneuvering system. This design must provide minimal resistance for longer durability during operation. In this study, the authors investigated the relationship between the distance, angle of attack, and shape of the NACA foil as a USV trimaran hull to reduce the resistance. The analysis began with verification and validation based on previous experimental research. Several configurations of the positions of each hull were modelled using an angle of attack of up to 20 °. Computational Fluid Dynamics (CFD) analysis was employed in ANSYS CFX to simulate the model. After obtaining the optimal configuration, variations in the NACA foil on the hull were performed, and the simulation was repeated. The study found that the configuration without an angle of attack, with one hull positioned in front and two hulls positioned behind, using NACA 0024 produces the smallest resistance value. Furthermore, this configuration exhibited wave interference with smaller volume-fraction contours. The study concludes that the angle of attack results in greater resistance owing to the shorter distance between the NACA foils. This research provides insight into the trimaran design of USVs and contributes to the further development of marine robotics technology and unmanned surface vehicles.

1. Introduction

Indonesia, with its vast and strategic area, boasts of abundant natural resources, making the defense of its outer borders vulnerable. As the largest archipelagic nation in the world, Indonesia has a long coastline to safeguard itself. Indonesia can consider participating in a multilateral security framework that will facilitate cooperation in all areas of security, including cyber technology [1]. Therefore, surveillance and exploration technologies are crucial for determining the conditions of

* *Corresponding author.*
E-mail address: fajri.ar@upnvj.ac.id (Fajri Ashfi Rayhan)

https://doi.org/10.37934/cfdl.15.11.3647

Indonesian territorial waters. Effective and fair management is required in accordance with local socio-ecological conditions to protect Indonesia's border ecosystems and ensure sustainable ecosystem services for Indonesian people [2]. An Unmanned Surface Vehicle (USV) is a technology that can minimize the risk of casualties while facilitating supervision and collecting data related to territorial areas in the waters. USVs are more flexible than large manned ships and can provide better solutions for data collection than survey ships. The use of survey ships is associated with low security, high costs, difficulty in data collection, and low chances of success, as reported by Sun *et al.,* [3].

Unmanned Surface Vehicles (USVs) are suitable tools for measuring sea data such as wave recording, hydrographic data, oceanographic data, and other sea measurements. USVs are a better option than large and costly research ships. Marine robots, such as USVs and Autonomous Underwater Vehicles (AUVs), are widely used in seabed mapping applications, oceanographic surveys, mine countermeasure operations, marine rescue, and environmental monitoring [4]. Recent studies by Li *et al.,* [5] and Song *et al.,* [6] introduce new methods for controlling the movement of USVs. Li *et al.,* [5] propose a 3D mapping and adaptive fuzzy control approach, which has proven effective in numerical experiments on the MATLAB platform, even in the presence of external disturbances. Similarly, Song *et al.,* [6] present a communication-efficient method in computer simulations for controlling unmanned boats to follow specific paths, even when the boat's behavior is uncertain. The latest USV design with the NACA foil as a hull form using a self-maneuvering system can provide a smaller resistance value, making it more durable. Recent research has also demonstrated that adopting the strategy of multiple diversion methods and nonlinear observer inhibition can effectively improve the convergent speed and tracking accuracy of USV formation trajectories. The permanent robustness of its MPC controller is combined to complete the observation and compensation of complex marine environment obstructions [7].

The NACA foil has been widely used in research related to the maximum lift force resulting from a geometric shape exposed to a fluid flow. This is because it has a lower resistance, making power usage more efficient and economical. Moreover, the NACA foil is also used for validation of numerical studies owing to the availability of experimental data for different profiles [8]. The foil profile shape is described using a series of numbers following the word "NACA.” For instance, the aerospace industry uses NACA foil for aircraft wing profiles, whereas the renewable energy industry employs it for wind turbine blades and water turbine impeller profiles [9].

Soğukpinar [10] conducted research on NACA foils in the aviation field by testing variations in the angle of attack for each NACA profile. It is known that the greater the angle, the greater the lift force; however, the change in the lift force becomes insignificant at an angle of 10 °. In other studies, related to energy, the heat-transfer performance of the NACA series foil fin Printed Circuit Heat Exchanger (PCHE) also increased as the foil thickness increased, but the comprehensive performance of the calculated flow and heat transfer decreased [11].

In addition to its applications in aviation and renewable energy industries, NACA foil is also utilized by naval architects to reduce the drag on ships and generate hydrofoil lift. Putranto and Sulisetyono [12] conducted research to determine the optimum characteristics of a hydrofoil, including maximum lift and drag reduction at a certain speed, minimum form factor, and avoidance of stall phenomenon. The NACA 4712, with an angle of attack of 15 °, met these criteria. Suastika *et al.,* [13] conducted research on the effect of using stern hydrofoil on ship resistance and found that at relatively low speeds (Fr ≤ 0.45), the use of stern foil increased ship resistance by up to 13%, while at relatively high speeds (Fr ≤ 0.55) it reduced the drag of the ship by up to 10%. For unmanned vessels with robotic automation systems, such as Micro Underwater Gliders (MUGs) that can operate with USVs, the best geometry is obtained using NACA 0016 with an angle of attack of 6.5 °because of its high ratio of lift and stall angle [14].

Azzeri *et al.,* [15] conducted a study on the resistance and the enforcement arm of the GZ of USV using a quantitative simulation method. Three variations of the hull distance with Froude number variations of 0.04 to 0.22 m/s were tested to obtain data on ship resistance. Additionally, a variation in the rotation angle from 0 °to 180 °was tested to obtain enforcement arm data. The study found that the widest hull spacing produced the least drag owing to wave interference. It was also reported that the value of the GZ enforcement arm at all hull distance variations complied with the International Maritime Organization (IMO) Code on Intact Stability [16]. Bahatmaka *et al.,* [16] simulated a mono-hull ship with varying deadrise angles. It was confirmed that the greater the deadrise angle, the lower is the resulting resistance. In another study, Naiem *et al.,* [17] analyzed the USV resistance with variations in the ship hull spacing using experimentation and simulation. Three variations in the distance between the hulls, with speed variations of 0.2 to 0.6 m/s were tested. It was found that the greater the distance between the hulls, the smaller is the ship resistance. However, based on a literature review, no study has yet been conducted on the effect of the type and angle of attack of NACA foil as a USV hull.

Therefore, the novelty of this study lies in conducting a numerical study on the resistance of a trimaran USV with an NACA foil-based hull. Simulation data were collected and validated using previous experimental studies. Finally, this study aimed to determine the minimum resistance data.

2. Fundamental Theory

Based on Birk [18], ship resistance is affected by the ship velocity, the weight of the water displaced by the submerged hull, and the ship hull shape. Ship resistance is denoted by RT, which stands for total resistance, with the equation:

$$RT = \frac{1}{2}\varepsilon \cdot \rho \cdot s \cdot {V_s}^2 \tag{1}$$

RT is total resistance [N], ε is ship total resistance coefficient [-], ρ is fluid density [kg/m^3], s is ship's wet surface area [m^2], Vs is ship velocity [m/s]

Ship friction resistance coefficient is regression equation to Reynold Number function.

$$C_F = \frac{0.075}{(\log{(Re)} - 2)^2} \tag{2}$$

C_F is friction resistance [-], Re is Reynolds Number [-] with equation:

$$R_e = \frac{V_S \cdot L}{\vartheta} \tag{3}$$

Re is Reynolds Number [-], Vs is ship velocity [m/s], L is the length of the ship [m], ϑ is kinematic viscosity [m^2/s].

The Reynolds-averaged Navier–Stokes equations (RANS equations) are the time-averaged motion equations for fluid flows. The idea behind the equations is the Reynolds decomposition, in which instantaneous quantities are decomposed into quantities averaging time and their fluctuations. The RANS equations were primarily used to describe turbulent flows. These equations can provide an estimate of the time-average solution to the Navier–Stokes equation using an approximation based on knowledge of the turbulence properties of the flow. For a stationary flow of an incompressible, Newtonian fluid, this equation can be written in Einstein notation in Cartesian coordinates as:

$$\rho\bar{u}_j\frac{\delta\bar{u}_i}{\delta x_j}=\rho\overline{f_i}+\frac{\delta}{\delta x_j}\left[-\bar{p}\delta_{ij}+\mu\left(\frac{\delta\bar{u}_i}{\delta x_j}+\frac{\delta\bar{u}_j}{\delta x_i}\right)-\rho\overline{u'_i u'_j}\right] \quad (4)$$

In this study, ANSYS CFX is used as a commercial CFD software to solve the Reynolds Average Navier-Stokes (RANS) equation. The RANS equation models the Reynolds shear stress in the N-S equation for inviscid, incompressible flow (except near walls). As for turbulence consideration, the realizable k - ε model is implemented, which is commonly used to analyze ship resistance. Scalar values of k and ε; k representing the turbulent kinetic energy, and ε representing the turbulent dissipation rate. On the other hand, Guan *et al.,* [19] utilized a different method for CFD simulation of USV by using STAR-CCM+ to solve RANS-VOF.

3. Research Method

The method involved in this study begins with creating a USV model, which will be simulated based on the main measurement data from previous studies (see Figure 1). Table 1 shows the dimensions of the trimaran that was studied by Naiem *et al.,* [17]. As for the hull design, the NACA Foil profile was chosen and designed using Autodesk Inventor. The three-dimensional trimaran ship models were created using Rhinoceros (see Figure 2).

Table 1
Dimensions of the trimaran [17]

Main Size	Unit (m)
Length Overall (LOA)	0,906
Beam Overall	0,820
Height	0,325
Draft	0,268

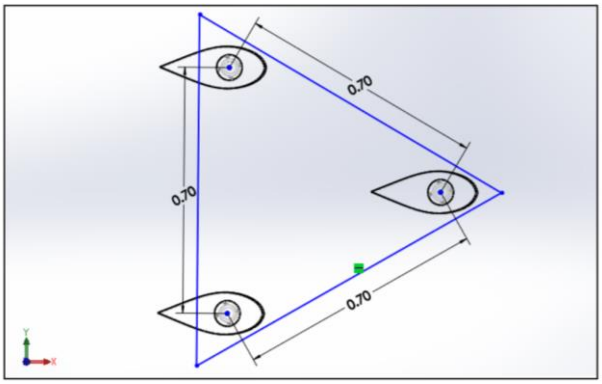

Fig. 1. Top view of trimaran ship USV

Fig. 2. Three-dimensional model trimaran ship USV

The next stage is to set the boundary of the trimaran model so that it can be simulated to resemble the conditions of the previous research. The boundary conditions were created using Ansys ICEM, with inlet limits for simulation extended to 1.50L at the front of the model and outlet limits set at 3.00L at the rear of the model. The portside and starboard limits were set at 1.85L each, and the limits under the keel were also set at 1.85L. Air layer or opening was extended 0.40L above the free surface. For more details, the boundary conditions can be seen in Figure 3. In the meshing settings, a density value of 0.1 was used for the boundaries, and 0.0033 was used for the trimaran ships to make them denser.

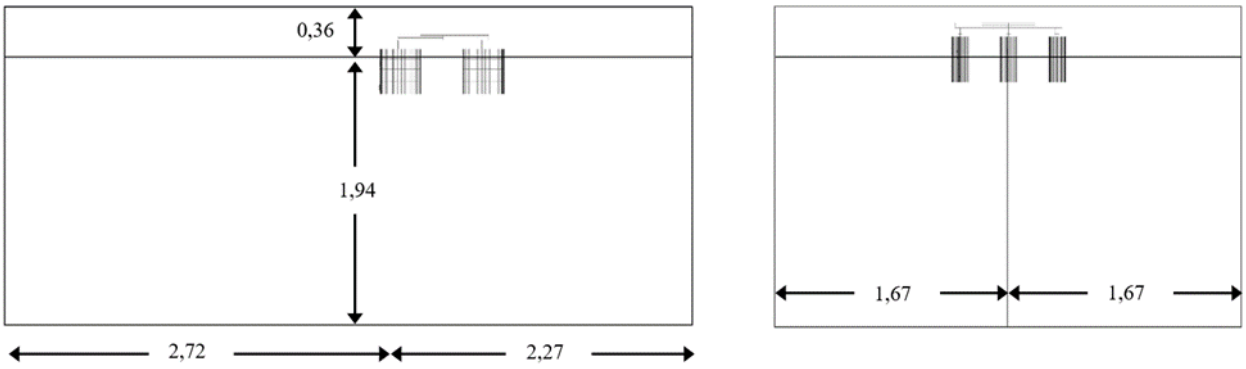

(a) (b)

Fig. 3. (a) Side view of boundary (b) Front view of boundary

To run the simulation on Ansys CFX, it is necessary to set the location classification for each component within the boundary conditions. The boundary conditions for each component were set to separate the domain into air and water domains with a temperature of 25°C and a pressure of 1 atm. The shear stress support was also adjusted. The water fluid velocity was set to equal the trimaran ship speed, while the air fluid velocity was set to zero. The outflow condition was set to average static pressure, and the open domain conditions were in accordance with the boundary conditions. The model conditions were then set to no slip wall with a smooth wall roughness level. After setting the boundary conditions and model conditions, the solver control details were adjusted. The convergent control was set to a maximum of 250 iterations, with a residual target of 0.0001.

After simulating the trimaran ship model on Ansys CFX, the meshing convergence decreases gradually from a total element mesh of 79,000 to a total element mesh of 139,000, as shown in the Figure 4.

After the convergence of the mesh has been carried out, the actual value of the experimental results to control for the relative error percentage still needs to be calculated to achieve research validation of the CFD analysis results as the initial stage of the design. The mean deviation equation is shown as follows:

$$MD = \frac{1}{N}\sum_{1}^{N}\left|(dpre - dexp).\frac{100}{dexp}\right| \quad (5)$$

Where MD is mean deviation [-], N is sum of data [-], $dpre$ is prediction data [N], and $dexp$ is experimental data [N].

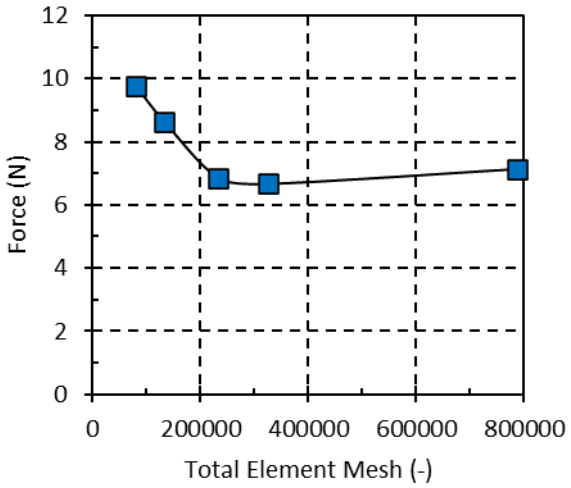

Fig. 4. The convergence graph of meshing values

Figure 5 displays the results of calculating the mean deviation. The simulation and experimental data yielded a mean deviation of 2,41%, satisfying the study's criteria. After the simulation data is valid, trimaran hull with NACA 0040 is made into six configurations. The configuration varies based on the position and angle of attack from each hull. Detailed configuration data is shown in Table 2 and Figure 6.

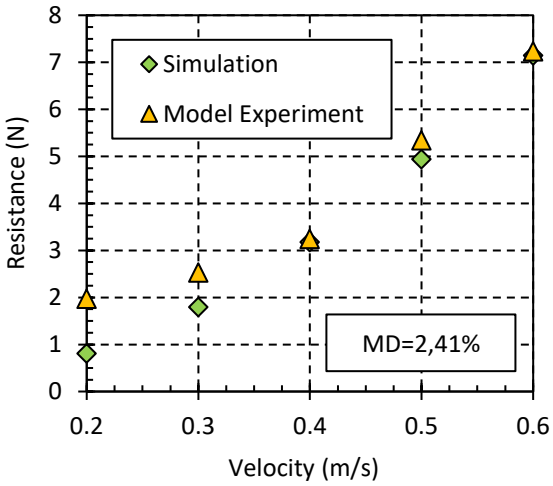

Fig. 5. Comparison graph of simulated and experimental resistance values

Table 2
Detailed configuration data

Configuration	Hull Spacing (m)	Hull Angle
Configuration 1	0,7	0°
Configuration 2	0,7	10°
Configuration 3	0,7	20°
Configuration 4	0,7	0°
Configuration 5	0,7	10°
Configuration 6	0,7	20°

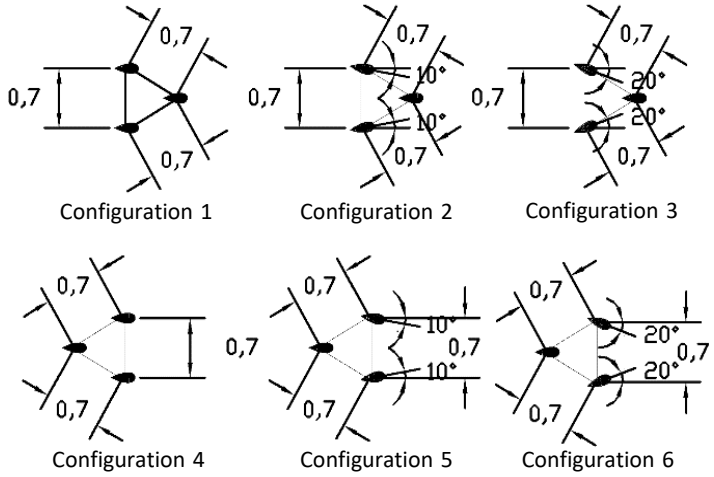

Fig. 6. Configuration setup detail

After finding the lowest resistance data between configurations 1 to 6, the next variation is to change the foil used to NACA 0024 and NACA 0032. Therefore, a summary of the variations in research data used is shown in Table 3.

Table 3
Summary of the variations in research data

Variation	Value			
Velocity (m/s)	0,2; 0,3; 0,4; 0,5; 0,6			
Main Size	Length (m)	Width (m)	Height (m)	Draft (m)
	0,906	0,820	0,325	0,268
Configuration	1-6			
NACA Foil	0040; 0024; 0032			

4. Results and Discussion

Based on the results of the resistance simulation carried out on configurations 1 to 6 at speeds ranging from 0.2 m/s to 0.6 m/s, Figure 7 is obtained as a comparison. From the figure, it can be seen that for the USV trimaran model using NACA 0040, the smallest resistance value is obtained in configuration 1. The highest resistance value is found in configuration 3, which has an average resistance value more than 4.94% higher than configuration 1. Configuration 3 uses the same NACA Foil arrangement as configuration 1, but with an angle of attack of 20°, making the foil position closer. Basically, the higher the angle of attack on the foil, the higher the resulting resistance. It is reported that an increase in the angle of attack above 5° will significantly increase the resistance, as the front part of the foil expands and the boundary layer of the flow thickens [20]. Soğukpinar [10] confirms that NACA with an angle of attack will produce significant lift force along with drag force. Overall, the results of this study are consistent with previous research that proves that increasing the distance between the hulls will result in less resistance [17].

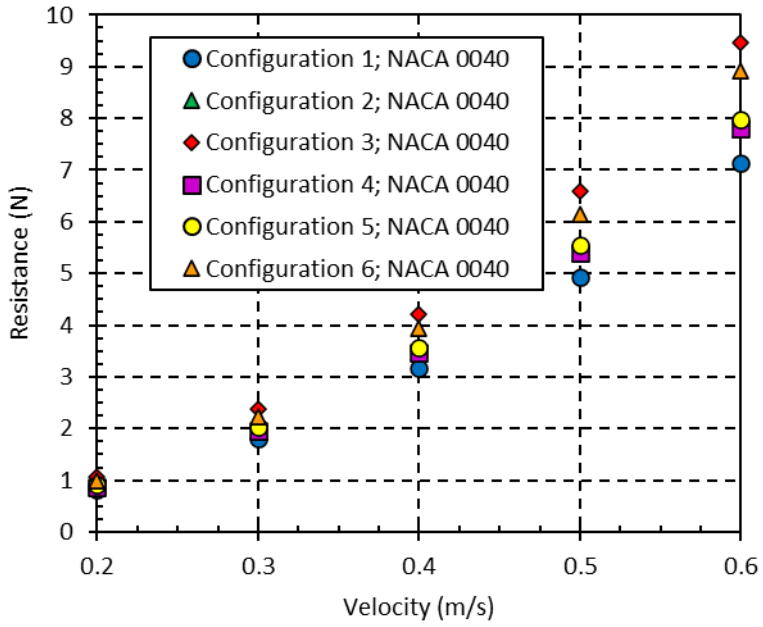

Fig. 7. Resistance vs velocity for NACA 0040

Once it was known that configuration 1 with NACA 0040 had the smallest resistance, variations were made by changing the shape of the hull of the USV trimaran ship (see Figure 8). NACA 0024 and NACA 0032 were used as the hulls. The best result was obtained with NACA 0024, which showed an average decrease in resistance value of 14,5% compared to configuration 1 using NACA 0040. Fundamentally, NACA 0024 produces lower resistance because it has a slimmer shape compared to NACA 0040 and NACA 0032. In previous research, there were two important principles that should be followed in designing an object to produce low resistance [21]: (i) if the object is long and thin, resistance can be reduced by smoothing the surface and maintaining laminar flow, and (ii) if the object is blunt, resistance can be reduced by streamlining and extending the rear part of the object.

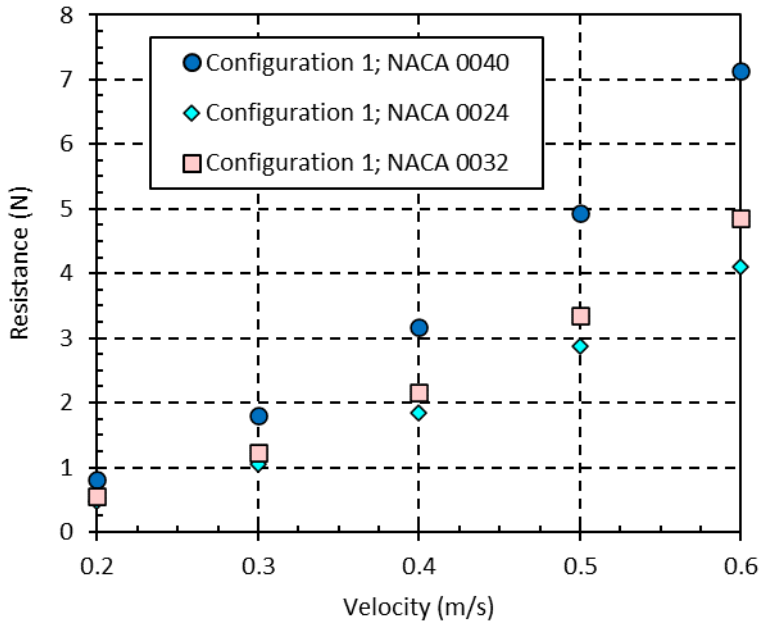

Fig. 8. Resistance comparison graph for configuration 1 with NACA variations

Based on Figure 9, it can be seen that overall, the non-dimensional unit of the total resistance coefficient (CT) for each configuration decreased. The lowest total resistance coefficient was found in the hull with configuration 1 using NACA 0024 variation, which was due to its low total resistance (RT) and small surface area. However, in previous research, a graph of the total resistance coefficient of an asymmetric trimaran ship showed an increase in CT when the ship speed was at Fr around 0.4 to 0.5 and a decrease when the ship speed was above 0,5 [22]. The difference in the rising and falling of the CT curve may be due to interference between wave systems, and thus a good hull design can ensure that the ship will operate at the desired speed conditions [23].

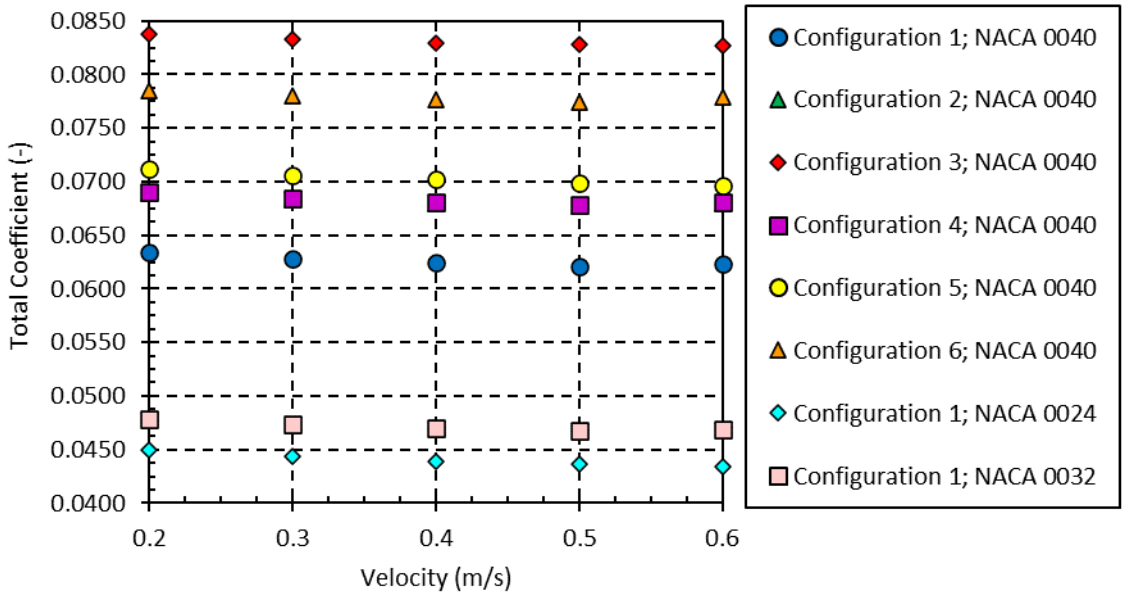

Fig. 9. Coefficient of total resistance comparison chart

The calculation results for the friction coefficient only show one graph of resistance because the USV model has the same length in every variation. As shown in Figure 10, the higher the speed of the trimaran, the lower the friction coefficient becomes. The decrease in the friction coefficient is caused by several factors, including: (i) wave shape that the ship passes through, (ii) shape of the ship's hull, (iii) surface area of the ship's hull that comes into contact with the fluid, (iv) vertical force of the hull against the fluid, (v) speed of the ship. However, the shape of the ship's hull and the surface area of the hull that comes into contact with the fluid are the most significant factors in this case. These two variables are the most significant factors because the trimaran uses NACA foil as its hull. NACA foil has a slender shape, making the frictional resistance experienced by the trimaran smaller. The decrease in the friction coefficient results in the trimaran being able to travel faster and perform its tasks more efficiently. If the friction coefficient becomes smaller, the resistance experienced by the ship also decreases. Hakim *et al.,* [24] conducted research on the frictional resistance experienced by their ship model, which increased as the ship's speed increased. This difference can occur because the ship model used in their study is a kriso container ship, and the fuel used is bio-fuel. The ship model used is different, so it is reasonable that there are differences in the calculation results. If one compares the container ship model used in the study by Hakim *et al.,* [24] with the ship model used by Naiem *et al.,* [17], differences in the number, slenderness, and hull shape can be observed. Another factor that causes differences in friction coefficient calculation results is the use of natural fuel. So far, the efficiency of natural fuel has not been able to surpass the efficiency of fossil fuels.

Therefore, the resulting speed decreases, causing the friction coefficient to increase, and ultimately, the resistance experienced by the ship also increases.

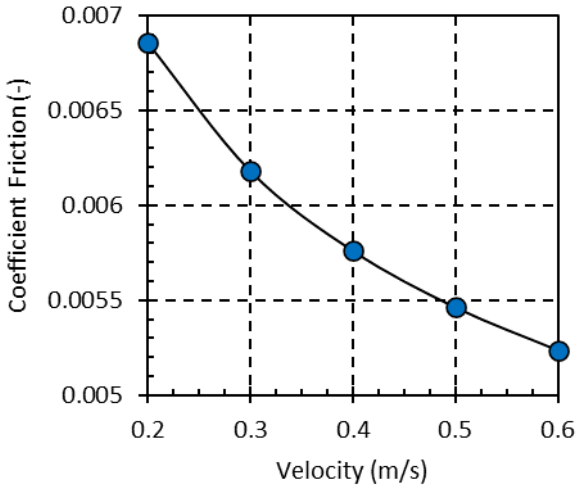

Fig. 10. Coefficient friction vs velocity

Figure 11 shows the contour of all configurations at a speed of 0.6 m/s resulting in a wave volume, namely the diffraction wave caused by the flow or water wave colliding against the surface of the trimaran USV model. The wave volume is indicated by the red to blue color. The red contour signifies a high-volume fraction value, while the blue contour signifies a low volume fraction value. The volume fraction is a representation of the space occupied by each phase, the law of conservation of mass and momentum filled by each fluid phase.

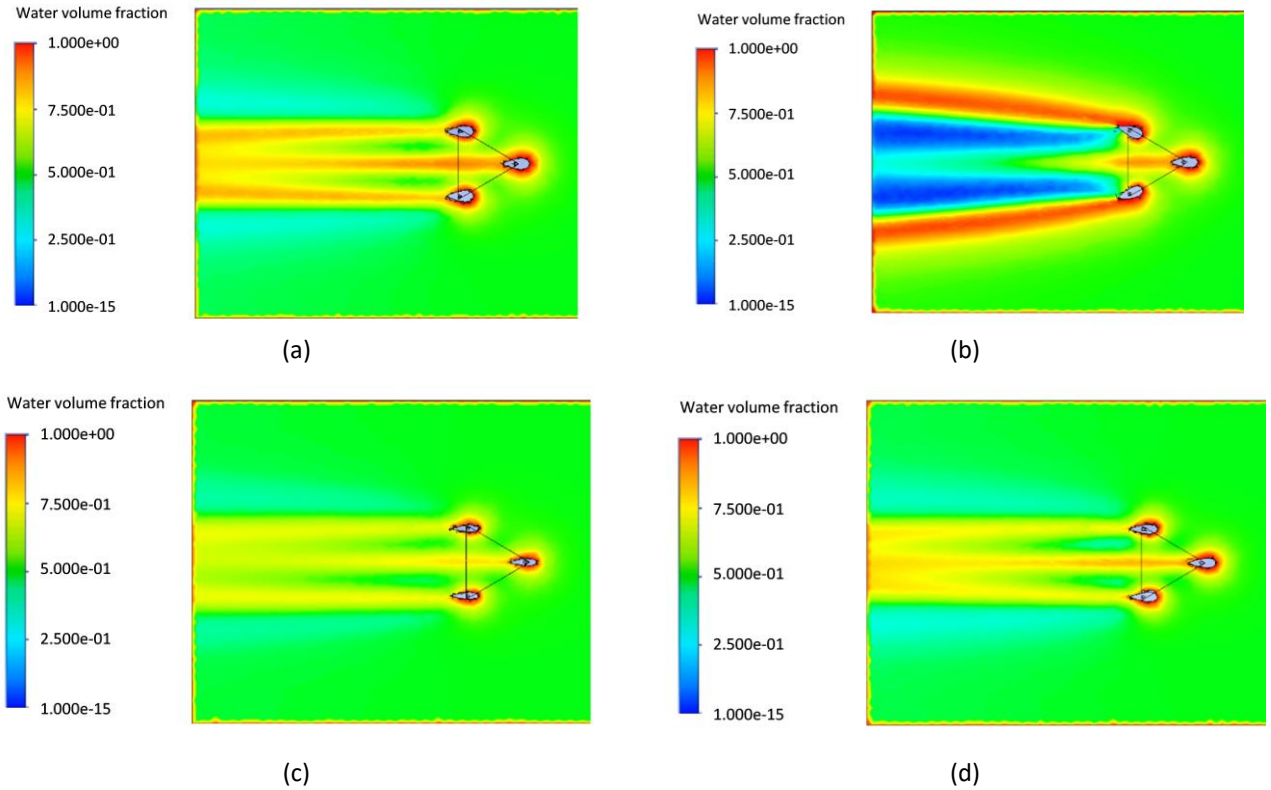

Fig. 11. USV trimaran wave contour (a) Configuration 1; NACA 0040 (b) Configuration 3; NACA 0040 (c) Configuration 1; NACA 0024 (d) Configuration 1; NACA 0032

In contour of configuration 1; NACA 0040 shows slight wave interference between the NACA, which is indicated by a pale-yellow colour that signifies a change in water volume fraction. Meanwhile, the contour of configuration 3; NACA 0040 produces a higher water volume fraction than other configurations, marked by a darker red colour due to the use of a higher angle of attack. A larger angle of attack results in a tighter distance between NACA, creating a greater wave interference. On the other hand, Samuel *et al.,* [25] reported that on a Deep-V Planning Hull, as the boat speed increases, the water volume fraction decreases. As the speed increases, the amount of air spreading beneath the hull increases due to the high trim value effect.

In configuration 1; NACA 0024 produces contours with the lowest volume fraction indicated by the absence of the colour red unlike in other configurations. Therefore, these results indicate that this configuration produces the lowest drag. In the same configuration, using NACA 0032 produces a higher volume fraction than the NACA 0024 variation, as indicated by darker shades of red and yellow.

5. Conclusions

This research was conducted using numerical simulations with the CFX ANSYS software. The simulation data were validated against previous studies conducted on USV trimarans. The variations in this study include the hull spacing, shape, and angle of attack of the NACA foil. In this study, the total drag of the ship, total drag coefficient, friction coefficient, and contour volume fraction of the trimaran USV ship were used as variables. Configuration 1 with NACA 0024 exhibited the lowest resistance, whereas configuration 3 with NACA 0040 demonstrated the highest resistance. It was concluded that the dimensions of the NACA, position of the NACA as the hull, and angle of attack of the trimaran affect the resistance value. This study contributes to the development of USV based on trimaran hull by providing valuable insights into their design. It is expected that these findings will help optimize the performance of USV trimaran vessels in real-world scenarios.

Acknowledgement

The authors would like to thank the UPNVJ USV research team. This work was supported by the Jakarta Veterans National Development University through the Scopus-Based Research (RISCOP) program with project number 145/UN.61.0/HK.07/LIT.RISCOP/2023.

References

[1] Zou, Yizheng. "China and Indonesia's responses to maritime disputes in the South China Sea: forming a tacit understanding on security." *Marine Policy* 149 (2023): 105502. https://doi.org/10.1016/j.marpol.2023.105502

[2] Fidler, Robert Y., Gabby N. Ahmadia, Amkieltiela, Awaludinnoer, Courtney Cox, Estradivari, Louise Glew et al. "Participation, not penalties: Community involvement and equitable governance contribute to more effective multiuse protected areas." *Science Advances* 8, no. 18 (2022): eabl8929. https://doi.org/10.1126/sciadv.abl8929

[3] Sun, Xu, Ling Zhang, Dalei Song, and QM Jonathan Wu. "A novel path planning method for multiple USVs to collect seabed-based data." *Ocean Engineering* 269 (2023): 113510. https://doi.org/10.1016/j.oceaneng.2022.113510

[4] Jia, Zehua, Haibo Lu, Shengquan Li, and Weidong Zhang. "Distributed dynamic rendezvous control of the AUV-USV joint system with practical disturbance compensations using model predictive control." *Ocean Engineering* 258 (2022): 111268. https://doi.org/10.1016/j.oceaneng.2022.111268

[5] Li, Jiqiang, Guoqing Zhang, Qihe Shan, and Weidong Zhang. "A novel cooperative design for USV-UAV systems: 3D mapping guidance and adaptive fuzzy control." *IEEE Transactions on Control of Network Systems* (2022). https://doi.org/10.1109/tcns.2022.3220705

[6] Song, Xiaona, Chenglin Wu, Vladimir Stojanovic, and Shuai Song. "1 bit encoding–decoding-based event-triggered fixed-time adaptive control for unmanned surface vehicle with guaranteed tracking performance." *Control Engineering Practice* 135 (2023): 105513. https://doi.org/10.1016/j.conengprac.2023.105513

[7] Dong, Zaopeng, Zhengqi Zhang, Shijie Qi, Haisheng Zhang, Jiakang Li, and Yuanchang Liu. "Autonomous Cooperative Formation Control of Underactuated USVs based on Improved MPC in complex ocean environment." *Ocean Engineering* 270 (2023): 113633. https://doi.org/10.1016/j.oceaneng.2023.113633
[8] Di Ilio, Giovanni, Daniele Chiappini, Stefano Ubertini, Gino Bella, and Sauro Succi. "Fluid flow around NACA 0012 airfoil at low-Reynolds numbers with hybrid lattice Boltzmann method." *Computers & Fluids* 166 (2018): 200-208. https://doi.org/10.1016/j.compfluid.2018.02.014
[9] Hetyei, Csaba, Ildikó Molnár, and Ferenc Szlivka. "Comparing different CFD software with NACA 2412 airfoil." *Progress in Agricultural Engineering Sciences* 16, no. 1 (2020): 25-40. https://doi.org/10.1556/446.2020.00004
[10] Soğukpinar, Haci. "Uçak Kanatlarinda En İdeal Hücum Açisini Bulmak İçin 4 Rakamli Naca 00xx Kanat Profillerinin Nümerik Analizi." *Uludağ Üniversitesi Mühendislik Fakültesi Dergisi* 22, no. 1 (2017): 169-178. https://doi.org/10.17482/uumfd.309470
[11] Chen, Fei, Lishen Zhang, Xiulan Huai, Jufeng Li, Hang Zhang, and Zhigang Liu. "Comprehensive performance comparison of airfoil fin PCHEs with NACA 00XX series airfoil." *Nuclear Engineering and Design* 315 (2017): 42-50. https://doi.org/10.1016/j.nucengdes.2017.02.014
[12] Putranto, Teguh, and Aries Sulisetyono. "Lift-drag coefficient and form factor analyses of hydrofoil due to the shape and angle of attack." *International Journal of Applied Engineering Research* 12, no. 21 (2017): 11152-11156.
[13] Suastika, Ketut, Affan Hidayat, and Soegeng Riyadi. "Effects of the application of a stern foil on ship resistance: A case study of an Orela crew boat." *International Journal of Technology* 8, no. 7 (2017): 1266-1275. https://doi.org/10.14716/ijtech.v8i7.691
[14] Elkolali, Moustafa, Wilfried Arnaud Splawski, Alfredo Carella, and Alex Alcocer. "Hydrodynamic parameter optimization for miniature underwater glider wings." In *Global Oceans 2020: Singapore–US Gulf Coast*, pp. 1-8. IEEE, 2020. https://doi.org/10.1109/ieeeconf38699.2020.9389187
[15] Azzeri, M. N., F. A. Adnan, M. Adi, and MZ Md Zain. "A concept design of three rudders-shaped like body in columns for low-drag USV." In *IOP Conference Series: Materials Science and Engineering*, vol. 133, no. 1, p. 012062. IOP Publishing, 2016. https://doi.org/10.1088/1757-899x/133/1/012062
[16] IMO, Resolution. "A749 (18)-Code on Intact Stability for all Types of Ships Covered by IMO Instruments." *International Maritime Organization* (1993).
[17] Naiem, Mohd Azzeri Md, Eizul Hanis Omar, Adi Maimun, Arifah Ali, Philip Wilson, Mohd Zarhamdy Md Zain, and Faizul Amri Adnan. "Drag analysis of three rudder-shaped like bodies." *Journal of Advanced Research in Fluid Mechanics and Thermal Sciences* 78, no. 1 (2021): 11-22. https://doi.org/10.37934/arfmts.78.1.1122
[18] Birk, Lothar. *Fundamentals of ship hydrodynamics: Fluid mechanics, ship resistance and propulsion*. John Wiley & Sons, 2019. https://doi.org/10.1002/9781119191575.ch1
[19] Guan, Guan, Lei Wang, Jiahong Geng, Zhengmao Zhuang, and Qu Yang. "Parametric automatic optimal design of USV hull form with respect to wave resistance and seakeeping." *Ocean Engineering* 235 (2021): 109462. https://doi.org/10.1016/j.oceaneng.2021.109462
[20] "Inclination Effects on Drag - Glenn Research Center." NASA, July 28, 2022.
[21] Hariyadi, Setyo. "An analysis on Aerodynamics Performance Simulation of NACA 23018 Airfoil Wings on Cant Angles." *JEMMME (Journal of Energy, Mechanical, Material, and Manufacturing Engineering)* 2, no. 1 (2017): 31-40. https://doi.org/10.22219/jemmme.v2i1.4905
[22] Yanuar, Yanuar, Gunawan Gunawan, Ibadurrahman Ibadurrahman, R. Ramadyan Mufti, and J. Wongso Putro. "Total hull resistance of asymmetrical trimaran model with hull separation and staggered hull variation of sidehull." In *AIP Conference Proceedings*, vol. 2255, no. 1. AIP Publishing, 2020. https://doi.org/10.1063/5.0020484
[23] Edward V. Lewis. "Principles of naval architecture second revision." *Jersey: Sname* 2 (1988): 152-157.
[24] Hakim, Muhammad Luqman, I. K. Suastika, and I. K. A. P. Utama. "A practical empirical formula for the calculation of ship added friction-resistance due to (bio) fouling." *Ocean Engineering* 271 (2023): 113744. https://doi.org/10.1016/j.oceaneng.2023.113744
[25] Samuel, Samuel, Sarjito Jokosisworo, Muhammad Iqbal, Parlindungan Manik, and Good Rindo. "Verifikasi Deep-V Planing Hull Menggunakan Finite Volume Method Pada Kondisi Air Tenang." *TEKNIK* 41, no. 2 (2020): 126-133. https://doi.org/10.14710/teknik.v0i0.29391